

Zn(II)-Benzotriazolate Clusters Based Amide Functionalized Porous Coordination Polymers with High CO₂ Adsorption Selectivity

Yong-Qiang Chen, Yang-Kun Qu, Guo-Rong Li, Zhan-Zhong Zhuang, Ze Chang,* Tong-Liang Hu, Jian Xu, and Xian-He Bu*

Department of Chemistry, TKL of Metal- and Molecule-Based Material Chemistry, and Collaborative Innovation Center of Chemical Science and Engineering (Tianjin), Nankai University, Tianjin 300071, China

Supporting Information

ABSTRACT: Two new porous coordination polymers (PCPs) based on different nanosized C₃ symmetry ligands and Zn(II)-benzotriazolate clusters have been synthesized solvothermally. Both of the desolvated complexes show selective uptake of CO₂ over CH₄ and N₂ at ambient temperature.

The emission of carbon dioxide (CO₂) has caused global warming and corresponding climate changes. Therefore, the reduction of CO₂ in the atmosphere becomes one of the greatest challenges worldwide.¹ Porous materials with high CO₂ sorption capacity and selectivity, especially in the low pressure range,^{1b} have been desired for potential applications. Recently, porous coordination polymers (PCPs) have received growing attention for their potential application in carbon capture and storage (CCS) due to their easily tailored structures, high stability, and permanent porosity with extra-high surface areas.² Along with the readily modulated pore structure, the pore surface properties of PCPs, which determined the interaction between the CO₂ molecules and host framework, were also found to be an important factor that affect the CCS performances of these materials.³ Up to now, several pore surface functionalization strategies have been proved to be effective.⁴ Generally, the functionalized materials reveal improved CO₂ capacity and selectivity due to the enhanced interactions between the active sites and CO₂ molecules.⁵

Among the various polar groups available for functionalization, the –CONH– group has been widely utilized to construct PCPs that exhibit strong CO₂ binding affinity.^{3,5,6} However, the flexible nature of this group may also reduce the porosity and the stability of the PCPs.⁷ Toward the construction of CCS targeted PCPs, we focused on two nanosized C₃ symmetry ligands with –CONH– polar groups, namely 4,4',4''-[1,3,5-benzenetriyltris(carboxylimino)]tris(benzoate) (H₃L1) and 3,3',3''-[1,3,5-benzenetriyltris(carboxylimino)]tris(benzoate) (H₃L2) for their potential to produce high porosity PCPs. On the other hand, Zn(II)-benzotriazolate (Zn-btz, btz = benzotriazolate) clusters were introduced as secondary building units (SBUs) in the targeted system, which could reduce the possibility of compact structures and increase the stability of the PCPs.⁸ Herein, we report two PCPs, {[Zn₅(L1)(btz)₆(H₂O)(NO₃)]·5DMA·5H₂O}_∞ (1) and {[Zn₉(L2)₂(btz)₁₂]·14H₂O}_∞ (2), based on the mentioned multidentate carboxylate ligands and two different Zn-btz clusters. These

PCPs reveal high porosity and remarkable CO₂/CH₄ and CO₂/N₂ selectivity, which meet the requirements as a candidate of CCS material.

Complex 1 was synthesized under solvothermal conditions with Zn(II) salt, btz, and H₃L1 as reactants. Single-crystal X-ray diffraction analysis revealed that 1 crystallizes in space group C2/c. In 1, Zn(II) ions exhibit three coordination modes; and six btz ligands link five Zn(II) ions to give a pentanuclear metal cluster with tetrahedral structure (Figure 1a). In the cluster,

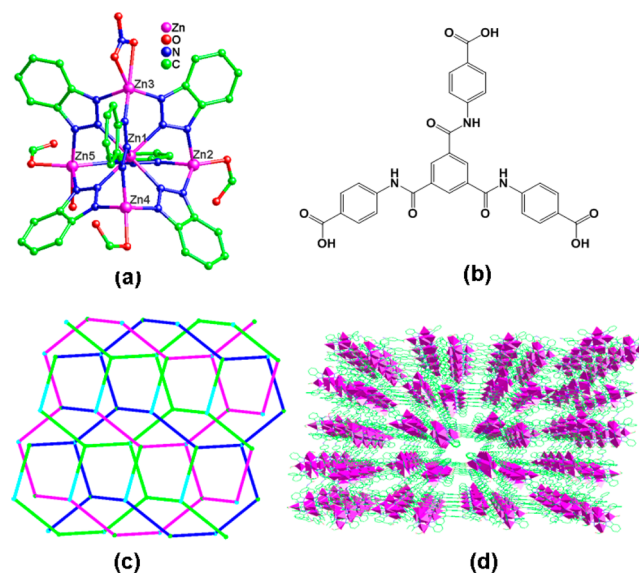


Figure 1. (a) The pentanuclear Zn(II) cluster in 1. (b) Schematic representation for the structure of the H₃L1 ligand. (c) Self-penetrating in the 2D network. (d) Polyhedral view of the stacked porous layers along the *b* axis.

four Zn(II) ions (Zn2, Zn3, Zn4, and Zn5) serve as vertices, and one Zn(II) ion (Zn1) is located at the center. Each vertex Zn(II) ion is linked to the other three through 1,3-bridge mode of the btz ligands. Besides the coordination of three N atoms, the four coordination environment of Zn2 and Zn4 ions is completed with one O atom from a carboxyl group, while the five coordination mode of Zn3 and Zn5 ions is completed with a chelating nitrate group and O atoms from a terminal H₂O and

Received: April 3, 2014

Published: August 13, 2014

and a monodentate carboxyl group, respectively. Furthermore, the pentanuclear units are linked by deprotonated $L1^{3-}$ ligands at the vertex positions (Figure 1b and Figure S1) to result in a porous 2D network (Figure S2a). By regarding the metal clusters and ligands as 3-connected nodes, the network of **1** can be rationalized as an unusual uninodal 3-c (10^3) net (Figure S2b), which has not been found in 2D networks. It should be noted that the 2D network shows a unique self-penetrating feature that is rarely reported (Figure 1c). In the crystal lattice, the 2D nets stack closely in an A–A mode along the *c* axis, and one-dimensional (1D) channels were formed in the *b* and *c* directions (dimensions $\approx 7.7 \times 7.8$ Å; Figure 1d and Figure S3).

Similar to that of complex **1**, the Zn centers in complex **2** show four-, five-, and six-coordination configuration (Figure 2a), while two pentanuclear clusters similar to that in **1** were

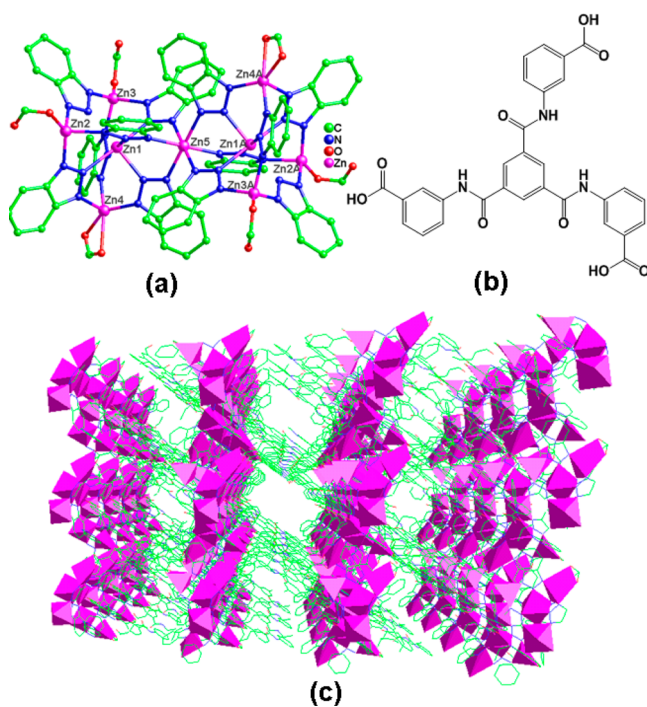


Figure 2. (a) The Zn_9 cluster. (b) Schematic representation for the structure of the H_3L_2 ligand. (c) Polyhedral view of the stacked porous network along the *b* axis.

connected by sharing one Zn ions to give a Zn_9 cluster. The neighboring Zn_9 units are connected by $L2^{3-}$ ligands to form a 2D network (Figure 2b, Figures S4 and S5a). The Zn_9 units and ligands could be regarded as 6- and 3-connected nodes, respectively, and, the overall 2D network of **2** can be rationalized as a (3,6)-c *kgd* net with Schläfli symbol $\{4^3\}_2\{4^6.6^6.8^3\}$ (Figure S5b). Moreover, the close stacking of the 2D nets in **2** leaves square shaped 1D channels along the *b* direction (dimensions $\approx 7.5 \times 7.6$ Å; Figure 2c and Figure S6).

Notably, the syntheses of complexes **1** and **2** were carried out using a one pot method, different from the previous reported stepwise synthesis of metal-benzotriazololate cluster based MOFs.⁹ These results show that the assembly of the Zn-btz clusters could be achieved in various conditions with different components, indicating the stability of this assembly system.

To prove our expectation on the enhancement of structure stability, thermogravimetric, PXRD, and porosity analyses were performed with complexes **1** and **2**. The results show that

complexes **1** and **2** are thermally stable up to 330 and 370 °C, respectively (Figures S7 and S8). The PXRD profiles of two complexes indicate that no significant change was observed for the host framework even though the guest solvent molecules were removed (Figures S9 and S10). The permanent porosity of activated complexes **1a** and **2a** were established by N_2 sorption experiments at 77 K, (Figures S11 and S12). The apparent Brunauer–Emmett–Teller (BET) and Langmuir surface areas are $421 \text{ m}^2\cdot\text{g}^{-1}$ for **1a** and $293 \text{ m}^2\cdot\text{g}^{-1}$ for **2a**. The mean pore size distribution is about 0.78 nm for **1a** and 0.75 nm for **2a**. These results indicate that compared to the related complex $[(Zn_4O)_2L_4(DMF)_2(H_2O)_3]\cdot 2.5H_2O$ ($L = L1$) constructed with the nanosized C_3 symmetry ligands,⁷ the incorporation of Zn-btz clusters can effectively enhance the structure stability.

H_2 sorption for complexes **1a** and **2a** was carried out to explore their potential storage application for this attractive energy carrier gas (Figures S13 and S14). The uptakes are ca. 0.75 wt % (77 K) and ca. 0.42 wt % (87 K) for **1a**, and ca. 0.68 wt % (77 K) and ca. 0.52 wt % (87 K) for **2a** around 1 atm. The adsorption enthalpies of H_2 were also estimated from the H_2 isotherms at 77 and 87 K by using a modified version of the Langmuir–Freundlich equation.¹⁰ The enthalpies of the adsorption are $13.8\text{--}10.8 \text{ kJ mol}^{-1}$ for **1a** and $11.2\text{--}8.3 \text{ kJ mol}^{-1}$ for **2a** (Figures S15–S18), which are substantially larger than that of many reported MOFs,^{10b,11} indicating the enhanced interaction between the pore surface and the hydrogen molecules adsorbed.

On the other hand, the enriched amide groups in complexes **1** and **2** encourage us to further examine their CCS behaviors. As shown in Figure 3, the uptakes of CO_2 are ca. $42.79 \text{ cm}^3 \text{ g}^{-1}$ at 273 K (STP, ca. 8.39 wt %) and ca. $25.96 \text{ cm}^3 \text{ g}^{-1}$ at 298 K (STP, ca. 5.08 wt %) for **1a**, while for **2a** the uptake amounts of CO_2 are ca. $46.23 \text{ cm}^3 \text{ g}^{-1}$ at 273 K (STP, ca. 9.02 wt %) and ca. $29.12 \text{ cm}^3 \text{ g}^{-1}$ at 298 K (STP, ca. 5.71 wt %). These capacities of CO_2 are better than those of the well-known MOF-5 (6.2 wt %, 273 K; 3.2 wt %, 298 K) and MOF-177 (3.6 wt %, 298 K).¹² However, only a limited amount of CH_4 are adsorbed under the same conditions. Furthermore, in the case of N_2 (273 and 298 K), almost no loading occurs. Moreover, the enthalpies of CO_2 adsorption were calculated using the modified Clausius–Clapeyron equation^{10b,13} (Figures S19–S24) by analyzing the isotherms at 273 and 298 K, respectively, and the values were found to be around $30.15 \text{ kJ mol}^{-1}$ for **1a** and around $35.23 \text{ kJ mol}^{-1}$ for **2a** depending on gas uptake, implying relatively strong interactions between CO_2 and the pore surfaces. The selective uptake of CO_2 over N_2 and CH_4 for two complexes and the significantly enhanced enthalpies could be mainly attributed to the significant quadrupole moment of CO_2 ($-1.4 \times 10^{-39} \text{ cm}^2$) and the presence of $-\text{CONH}-$ groups in complexes **1** and **2**, which could facilitate dipole–quadrupole interactions.^{6a} Furthermore, the CO_2/N_2 and CO_2/CH_4 adsorption selectivities of two complexes at 273 K were calculated from the experimental single component isotherms using ideal adsorbed solution theory (IAST)^{6a,14} (Figure S25). The CO_2/N_2 selectivities calculated for a 15/85 CO_2/N_2 mixture are 79 and 186 for **1** and **2** at 1 atm, and the CO_2/CH_4 selectivities calculated for a 50/50 CO_2/CH_4 mixture are 8 and 12 for **1** and **2** at 1 atm, respectively. These results are comparable with many reported MOFs.^{5,6} The selective adsorptions of CO_2 over CH_4 and N_2 promise that they may be applied in natural gas purification for energy production and greenhouse gas capture purposes.

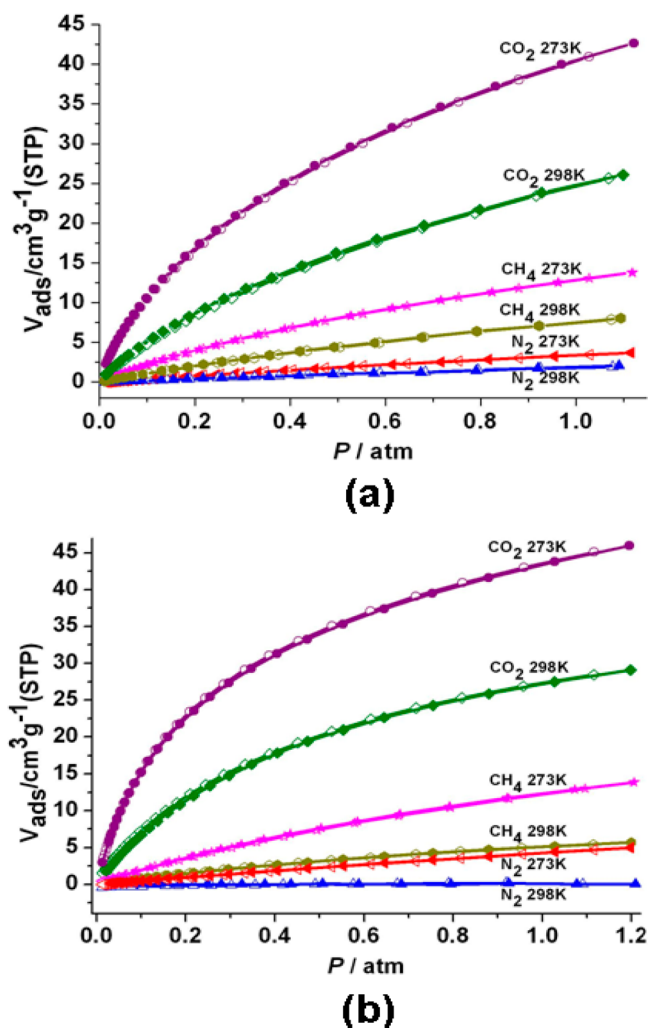


Figure 3. Sorption isotherms of CO₂, CH₄, and N₂ measured at 273 and 298 K, respectively, (a) for 1a and (b) for 2a.

In conclusion, two new microporous PCPs with –CONH– functional sites have been rationally constructed based on nanosized C₃ symmetry ligands and Zn(II)-benzotriazolate clusters. Both of them exhibit highly selective uptake for CO₂ over CH₄ and N₂ near room temperature, which is promising for their utilization in CO₂ capture and storage.

ASSOCIATED CONTENT

Supporting Information

Crystallographic details (CIF), experimental section, supplementary tables, structural figures, and additional characterizations. This material is available free of charge via the Internet at <http://pubs.acs.org>.

AUTHOR INFORMATION

Corresponding Authors

*Fax: +86-22-23502458. E-mail: changze@nankai.edu.cn.

*Fax: +86-22-23502458. E-mail: buxh@nankai.edu.cn.

Notes

The authors declare no competing financial interest.

ACKNOWLEDGMENTS

This work was supported by the 973 Program of China (2012CB821700 and 2014CB845600), the National Science

Foundation of China (21031002, 21290171, and 21202088), and MOE Innovation Team (IRT13022) of China.

REFERENCES

- (a) Liu, J.; Thallapally, P. K.; McGrail, B. P.; Brown, D. R.; Liu, J. *Chem. Soc. Rev.* **2012**, *41*, 2308–2322. (b) Nagarkar, S. S.; Chaudhari, A. K.; Ghosh, S. K. *Inorg. Chem.* **2012**, *51*, 572–576. (c) *IPCC Special Report on Carbon Dioxide Capture and Storage*; Cambridge University Press: Cambridge, U.K., 2005. (d) Chen, Q.; Chang, Z.; Song, W. C.; Song, H.; Song, H. B.; Hu, T. L.; Bu, X. H. *Angew. Chem., Int. Ed.* **2013**, *52*, 11550–11553.
- (a) Luebke, R.; Eubank, J. F.; Cairns, A. J.; Belmabkhout, Y.; Wojtas, L.; Eddaoudi, M. *Chem. Commun.* **2012**, *48*, 1455–1457 and references therein. (b) Qin, J. S.; Du, D. Y.; Li, W. L.; Zhang, J. P.; Li, S. L.; Su, Z. M.; Wang, X. L.; Xu, Q.; Shao, K. Z.; Lan, Y. Q. *Chem. Sci.* **2012**, *3*, 2114–2118. (c) Tian, D.; Chen, Q.; Li, Y.; Zhang, Y. H.; Chang, Z.; Bu, X. H. *Angew. Chem., Int. Ed.* **2014**, *53*, 837–841.
- (a) Duan, J. G.; Yang, Z.; Bai, J. F.; Zheng, B. S.; Li, Y. Z.; Li, S. H. *Chem. Commun.* **2012**, *48*, 3058–3060 and references therein.
- (a) For example: (a) Demessence, A.; D'Alessandro, D. M.; Foo, M. L.; Long, J. R. *J. Am. Chem. Soc.* **2009**, *131*, 8784–8786. (b) Yang, E.; Li, H. Y.; Wang, F.; Yang, H.; Zhang, J. *CrystEngComm* **2013**, *15*, 658–661 and references therein. (c) Wang, F.; Tan, Y. X.; Yang, H.; Kang, Y.; Zhang, J. *Chem. Commun.* **2012**, *48*, 4842–4844. (d) Lin, R. B.; Chen, D.; Lin, Y. Y.; Zhang, J. P.; Chen, X. M. *Inorg. Chem.* **2012**, *51*, 9950–9955. (e) Wang, X. J.; Li, P. Z.; Liu, L.; Zhang, Q.; Borah, P.; Wong, J. D.; Chan, X. X.; Rakesh, G.; Li, Y. X.; Zhao, Y. L. *Chem. Commun.* **2012**, *48*, 10286–10288.
- (a) Zheng, B. S.; Yang, Z.; Bai, J. F.; Li, Y. Z.; Li, S. H. *Chem. Commun.* **2012**, *48*, 7025–7027.
- (a) Zheng, B. S.; Bai, J. F.; Duan, J. G.; Wojtas, L.; Zaworotko, M. J. *J. Am. Chem. Soc.* **2011**, *133*, 748–751. (b) Zou, Y.; Park, M.; Hong, S.; Lah, M. S. *Chem. Commun.* **2008**, 2340–2342. (c) Patel, H. A.; Yavuz, C. T. *Chem. Commun.* **2012**, *48*, 9989–9991. (d) Hasegawa, Y.; Horike, S.; Matsuda, R.; Furukawa, S.; Mochizuki, K.; Kinoshita, Y.; Kitagawa, S. *J. Am. Chem. Soc.* **2007**, *129*, 2607–2614. (e) Hou, C.; Liu, Q.; Fan, J.; Zhao, Y.; Wang, P.; Sun, W. Y. *Inorg. Chem.* **2012**, *51*, 8402–8408. (f) Chen, M. S.; Chen, M.; Takamizawa, S.; Okamura, T.; Fan, J.; Sun, W. Y. *Chem. Commun.* **2011**, *47*, 3787–3789.
- (a) Song, X. K.; Zou, Y.; Liu, X. F.; Oh, M.; Lah, M. S. *New J. Chem.* **2010**, *34*, 2396–2399.
- (a) Li, Y. W.; Li, J. R.; Wang, L. F.; Zhou, B. Y.; Chen, Q.; Bu, X. H. *J. Mater. Chem. A* **2013**, *1*, 495–499 and references therein.
- (a) Lan, Y. Q.; Li, S. L.; Jiang, H. L.; Xu, Q. *Chem.—Eur. J.* **2012**, *18*, 8076–8083 and references therein. (b) Wang, X. L.; Qin, C.; Wu, S. X.; Shao, K. Z.; Lan, Y. Q.; Wang, S.; Zhu, D. X.; Su, Z. M.; Wang, E. B. *Angew. Chem., Int. Ed.* **2009**, *48*, 5291–5295.
- (a) Tedds, S.; Walton, A.; Broom, D. P.; Book, D. *Faraday Discuss.* **2011**, *151*, 75–94. (b) Zhong, D. C.; Lin, J. B.; Lu, W. G.; Jiang, L.; Lu, T. B. *Inorg. Chem.* **2009**, *48*, 8656–8658.
- (a) Guo, Z. Y.; Li, G. H.; Zhou, L.; Su, S. Q.; Lei, Y. Q.; Dang, S.; Zhang, H. J. *Inorg. Chem.* **2009**, *48*, 8069–8071.
- (a) Deng, H.; Doonan, C. J.; Furukawa, H.; Ferreira, R. B.; Towne, J.; Knobler, C. B.; Wang, B.; Yaghi, O. M. *Science* **2010**, *327*, 846–850. (b) Rowsell, J. L. C.; Millward, A. R.; Park, K. S.; Yaghi, O. M. *J. Am. Chem. Soc.* **2004**, *126*, 5666–5667. (c) Millward, A. R.; Yaghi, O. M. *J. Am. Chem. Soc.* **2005**, *127*, 17998–17999.
- (a) Daniels, F.; Williams, J. W.; Bender, P.; Alberty, R. A.; Cornwell, C. D. *Experimental Physical Chemistry*; McGraw-Hill Book Co., Inc.: New York, 1962.
- (a) Bae, Y. S.; Mulfort, K. L.; Frost, H.; Ryan, P.; Punnathanam, S.; Broadbelt, L. J.; Hupp, J. T.; Snurr, R. Q. *Langmuir* **2008**, *24*, 8592–8598.